Published in final edited form as:
Biochemistry. 2011 May 10; 50(18): 3796–3806. doi:10.1021/bi101633b.

Heterogeneous nuclear ribonucleoprotein K and nucleolin as transcriptional activators of the vascular endothelial growth factor promoter through interaction with secondary DNA structures

Diana J. Uribe[2], **Kexiao Guo**[1], **Yoon-Joo Shin**[1], and **Daekyu Sun**[1,2,*]

[1] Pharmacology and Toxicology Department, University of Arizona, Tucson, AZ, 85721

[2] Cancer Biology Graduate Interdisciplinary Program, University of Arizona, Tucson, AZ, 85721

Abstract

The human vascular endothelial growth factor (VEGF) promoter contains a polypurine/polypyrimidine (pPu/pPy) tract that is known to play a critical role in its transcriptional regulation. This pPu/pPy tract undergoes a conformational transition between B-DNA, single stranded DNA and atypical secondary DNA structures such as G-quadruplexes and i-motifs. We studied the interaction of the cytosine-rich (C-rich) and guanine-rich (G-rich) strands of this tract with transcription factors heterogeneous nuclear ribonucleoprotein (hnRNP) K and nucleolin, respectively, both *in vitro* and *in vivo* and their potential role in the transcriptional control of VEGF. Using chromatin immunoprecipitation (ChIP) assay for our *in vivo* studies and electrophoretic mobility shift assay (EMSA) for our *in vitro* studies, we demonstrated that both nucleolin and hnRNP K bind selectively to the G- and C-rich sequences, respectively, in the pPu/pPy tract of the VEGF promoter. The small interfering RNA (siRNA)-mediated silencing of either nucleolin or hnRNP K resulted in the down-regulation of basal VEGF gene, suggesting that they act as activators of VEGF transcription. Taken together, the identification of transcription factors that can recognize and bind to atypical DNA structures within the pPu/pPy tract will provide new insight into mechanisms of transcriptional regulation of the VEGF gene.

Keywords

hnRNP K; nucleolin; VEGF; G-quadruplex; i-motif

Vascular endothelial growth factor (VEGF) has been recognized as one of the main factors required for new blood vessel formation in early tumorgenesis as well as in tumor invasion (1). VEGF overexpression is also observed in many clinically important solid tumors, suggesting its strong association with the progression and metastasis of cancer (2). Previous studies have identified a polypurine/polypyrimidine (pPu/pPy) tract, −85 to −50 relative to the transcription start site, as a main *cis*-element involved in the regulation of transcription

*Corresponding Author. Mailing address: BIO5 Institute, 1657 E. Helen St., Tucson, Arizona 85721. Phone: (520) 626-0323. Fax: (520) 626-4824. sun@pharmacy.arizona.edu.

†This work was funded by the National Institutes of Health (CA109069). Diana J. Uribe is a recipient of a Minority Supplement Grant (CA109069) provided by the Research Supplements to Promote Diversity in Health Related Research program at the National Institutes of Health.

SUPPORTING INFORMATION AVAILABLE

The effect of VEGF mRNA and protein levels upon knockdown of nucleolin, hnRNP K, CNBP and SP1 were verified using qPCR and western blot. This material is available free of charge via the Internet at http://pubs.acs.org.

activity of the VEGF gene (see Figure 1). Recently, our studies demonstrated that guanine and cytosine-rich (G- and C-rich) strands of this pPu/pPy tract are capable of forming alternative secondary DNA structures, G-quadruplexes and i-motifs respectively, when in the single-stranded state (3). A single-stranded state of this tract is believed to be achieved through transcription-generated dynamic supercoiling, which is leaving the DNA upstream of the event negatively supercoiled, or under-wound, and the DNA downstream positively supercoiled (3, 4). The dynamic character of this region would allow the G- and C-rich strands to form atypical non-B-DNA structures such as G-quadruplexes and i-motifs. The G-quadruplex structure consists of square planes of four guanines, called tetrads, held together by Hoogsteen hydrogen bonding (5, 6). Monovalent cations, such as potassium, stabilize the tetrads allowing them to stack, forming the base conformation of the G-quadruplex. In previous studies, we determined that the G-rich sequence of the VEGF promoter is able to form a parallel G-quadruplex structure with a 1:4:1 loop configuration *in vitro* (3).

Within the pPu/pPy tract of the VEGF promoter, Sp1 has been described as a major ubiquitously expressed transcription factor that recognizes the duplex form of this tract. There are known Sp1 binding sites within and outside of this pPu/pPy tract that influence VEGF transcription (7–11). Furthermore, the deletion of the pPu/pPy tract from the VEGF promoter is known to result in downregulation of transcription activity by 90% (8). We recently reported that nucleolin can bind selectively and with high affinity to VEGF G-quadruplex structures *in vitro* (12). This same article also demonstrated that nucleolin binds to the *c-myc* G-quadruplex which forms in the proximal promoter *in vitro* and that increasing the amounts of nucleolin expression leads to decreased *c-myc* transcription. This raises the possibility that nucleolin could regulate the transcription of the VEGF gene by binding to the G-quadruplex-forming region of this gene promoter *in vivo*.

Like the G-rich strand, the complementary C-rich strand in the pPu/pPy tract is also known to form intermolecular or intramolecular four-stranded i-motif structures *in vitro*. These unique secondary DNA structures are stabilized by the two parallel-stranded cytosine-cytosine (C–C+) base-paired duplexes (one cytosine must be hemi-protonated at the N3 position) that intercalate into each other in an antiparallel orientation (13). We have described the i-motif structure formed by the C-rich strand of the pPu/pPy tract in the VEGF promoter *in vitro*. This structure was proposed to have six $C\text{-}C^+$ intercalated base pairings with a 2:3:2 loop configuration under acidic conditions (3). In addition, circular dichroism (CD) analysis in the same study has identified the VEGF i-motif as pH dependent, with a transitional pH around 6.0. However, the hypothesis of the formation of the i-motif structure *in vivo* has been received with much skepticism in the scientific community, since the formation of the i-motif is heavily dependent on the hemi-protonation of cytosines to achieve C-C+ base-pairing, which is only accomplished below a physiologically relevant pH (14). Therefore, the discovery of the i-motif structure in the C-rich strand of the VEGF promoter prompted us to investigate whether this structure is able to form under physiological conditions as well as acidic conditions.

In addition, our efforts have focused on characterizing proteins that could potentially interact with secondary DNA structures formed in the C- and G-rich strands in the transcriptionally essential pPu/pPy tract of the VEGF promoter. Substantial evidence has shown that the human heterogeneous nuclear ribonucleoprotein K (hnRNP K) is known to bind preferentially to single-stranded C-rich sequences (15, 16). Most importantly, hnRNP K has been shown to be an activating transcription factor for the *c-myc* promoter (17, 18). Since hnRNP K is known to bind to the C-rich sequence in the nuclease hypersensitive element III_1 ($NHEIII_1$) region of the *c-myc* promoter, this protein was chosen as a candidate transcription factor which may recognize the C-rich strand in the pPu/pPy tract of the VEGF promoter. As stated earlier, nucleolin was recently described as a protein selectively binding

to the VEGF G-quadruplex (12). We investigated whether nucleolin could bind to the G-rich strand in the pPu/pPy tract of the VEGF promoter and determine the consequences of this *in vivo* binding of the protein to the transcriptional control of VEGF.

The results of our present study revealed that the transcription factors, hnRNP K and nucleolin, interact with the C- and G-rich strands, respectively, in the pPu/pPy tract of the VEGF promoter both *in vitro* and *in vivo*. The results also confirm that hnRNP K and nucleolin act as transcriptional activators of the VEGF gene which take part in the multi-structural DNA environment to coordinate and mediate VEGF transcription as in the case of the well characterized *c-myc* (17–19).

Methods and Materials

Purification and End-labeling of Oligonucleotide

A 24bp oligo containing the VEGF C-rich region (VC24) 5′-GACCCCGCCCCC GGCCCGCCCCGG-3′ as well as a 47bp oligo containing the complementary G-rich region (VG47) 5′-GCCCCCCGGGGCGGGCCGGGGGCGGGGT CCCGGCGGGGCGGAGCCAT-3′ were purchased from Sigma Genosys (The Woodlands, TX) and radiolabelled. 1μL of 100μM oligo was labeled with 30μCi of γ-^{32}P ATP, 10U of T4 polynucleotide kinase, 1× T4 kinase buffer and left to react at 37°C for at least 1 hour. The mixture was cleaned of unincorporated radioactive γ-^{32}P ATP with Micro Bio-Spin™ 30 columns (Bio-Rad, Hercules, CA) and gel purified using a 12% denaturing polyacrylamide-urea gel to separate the full-length product from all other contaminants. The full-length band was then excised from the gel, crushed and eluted with deionized water overnight at 37°C. The concentration was determined by absorbance measurements at 260nm using the nearest-neighbor method to calculate the molar extinction coefficient for each oligo according to its composition. The calculated extinction coefficient for the VC24 oligo is 198300(L/mol*cm) and 425400(L/mol*cm) for the VG47 oligo at 260nm (20).

Cell Culture

The human renal cell carcinoma cell line A498 and the human glioma cell line U251 were obtained from the American Type Culture Collection (Manassas, VA). The human embryonic immortalized kidney cells HEK293T were a gift from Dr. Margaret Briehl (Arizona Cancer Center, Tucson, AZ). ATCC and Thermo Scientific stated genotypic and phenotypic testing was done to validate cell line authenticity in the certified reference material provided with each cell culture. The A498 and U251 cell lines were cultured in RPMI 1640 media (Cellgro, Manassas, VA) and the HEK293T in DMEM, each supplemented with 10% heat-inactivated fetal bovine serum in a humidified atmosphere containing 5% CO_2 at 37 °C. Each cell line tested negative for mycoplasma contamination prior to and after experimentation.

Bromine Footprint of i-motif Structure

The cytosine specific probing procedure was adapted from a previous study that developed a method to chemically probe non-duplexed cytosine bases (21). The bromine footprints for i-motif structure characterization were performed using the pure 5′-end-labeled VC24 oligo in 140mM KCl, 50mM NaCl, and 10mM sodium-acetate (NaOAC) buffer at pH 4.3, 5.3, 6.1, 7.1 and 8.0. This mixture was then reacted with a molecular bromine solution which contained equal molar concentrations of $KHSO_5$ and KBr, for a final 50mM bromine stock solution, for 30 minutes at room temperature. Bromine reactivity decreases in alkaline solution, therefore we used increased bromine concentrations at higher pH levels. The bromine reaction was stopped with 5 to 10ug of calf thymus DNA and 300mM NaOAc following an ethanol precipitation/purification for each sample. The DNA mixture was dried

and cleaved via piperidine treatment using a 1:10 diluted solution and heated at 95°C for 30 minutes. After piperidine treatment, the samples were dried and washed with diH_2O twice. For quantifying purposes, each sample was resuspended in alkaline dye (80% formaldehyde, 10mM EDTA (pH 8.0), 1mg/mL xylene cyanol and bromophenol blue) so that the final radiation count per volume of each sample is 1kcpm/μL. 3–4kcpm of each sample was loaded and run in a 20% denaturing polyacrylamide sequencing gel, dried and exposed to a phosphor screen (Bio-Rad) and read on a STORM 860 Scanner (GE Healthcare Life Sciences, Pittsburgh, PA) for analysis.

Chromatin Immunoprecipitation Assay (ChIP)

The chromatin immunoprecipitation assays were performed as described previously (22) with slight modifications. A498 cells were cultured and cross-linked by the addition of formaldehyde, lysed, sonicated and the resulting supernatant was purified. The samples were reverse cross-linked and were purified using a Qiagen (Valencia, CA) PCR purification kit according to the manufacturer's instructions and used for PCR. The PCR primers used to amplify the VEGF proximal promoter region are forward primer (5′-GGTCGAGCTTCCCCTTCA-3′) and reverse primer (5′-GATCCTCCCCGCTACCAG-3′) (11). The PCR primers used to amplify the HIF1-α binding site known as the hypoxia response element (HRE) in the far upstream region of the VEGF promoter are forward primer (5′-GGAACAAGGGCCTCTGTCTG-3′) and reverse primer (5′-GAGAAGAATTTGGCACCAAG-3′). Forty cycles were used to amplify both regions of interest using the following PCR protocol; 95°C for 30 seconds, 52°C for 30 seconds, and 72°C for 30 seconds, in the presence of 2 mM magnesium chloride using Taq polymerase (Fermentas, Glen Burnie, Maryland). The VEGF proximal promoter region is very GC-rich, thus 6% DMSO and 1 M betaine were added to enhance the amplification of this region.

siRNA Treatment and Semiquantitative Reverse Transcription-PCR

A498, U251 and HEK293T cells were seeded into 6-well plates one day prior to transfection in complete RPMI 1640 or DMEM medium with 10% FBS. At the time of transfection with siRNAs, the cells were approximately 75% confluent and were transfected with siRNA (50 and 100nM) using RNAiMax (Invitrogen) in a serum-containing medium according to the manufacturer's protocol. The controls included transfection reagent without any siRNA, or with non-targeting siRNA. 48 hours after transfection, total mRNA was harvested from the treated cells and was subject to Reverse Transcriptase-PCR. Total RNA was isolated by using RNeasy Mini Kit (Qiagen) following the manufacturer's protocol with the Qiashredder to homogenize the cell tissue. Five-hundred nanograms of total RNA were reverse-transcribed in a total volume of 20μl using the qScript cDNA synthesis kit (Quanta Biosciences, Gaithersburg, MD), following the manufacturer's instructions. After reverse transcription, the cDNA was diluted 2X in 10mM Tris-HCl (pH 8.0) and subjected to PCR amplification using 2X Mastermix (Fermentas, Glen Burnie, MD) and nucleolin, hnRNP K, VEGF and Actin primers. Non-targeting siRNA and siRNA against nucleolin (C-23) and hnRNP K were purchased from Santa Cruz Biotechnology, Inc. (Santa Cruz, CA). Optimization experiments were done to achieve the strongest knock-out effect for each transcription factor and their gene family members. The list of primers used are as follows:

Nucleolin primers forward 5′-AGAAGGGAGCCACACCAGGC-3′ and reverse 5′-AGCTGCTGCTTTCATCGCTG-3′,

hnRNP K primers forward 5′-AATGGRGAATTTGGTAAACGCC-3′ and reverse 5′-TTTAGCACCTTTGACCCCAATAAT-3′

VEGF primers forward 5′-CGAAGTGGTGAAGTTCATGGATG-3′ and reverse 5′-TTCTGTATCAGTCTTTCCTGGT-3′, and

Actin primers forward 5′-TTCCTGGGCATGGAGTCCTGTGG-3′ and reverse 5′-CGCCTAGAAGCATTTGCGGTGG-3′.

Transient transfection of nucleolin and hnRNP K expression plasmids

The pEGFP-C3 control vector and the pEGFP-Nuc vector were a gift from Dr. Michael B. Kastan (St. Jude Children's Research Hospital) (23). The hnRNP K expression vector, pGFP-hnRNPK, was a gift from Dr. Rama Natarajan (Beckman Research Institute of City of Hope) (24). The vectors were transfected into the cultured A498, U251 and HEK293T cells by the standard cationic liposome transfection method according to the manufacturer's instructions (Turbo-Fect, Fermentas). The cells were harvested after 48 hours, lysed and the RNA purified using Qiagen's RNeasy Mini Kit. The RNA was reverse-transcribed using qScript cDNA Synthesis Kit (Quanta) following the manufacturer's protocol and amplified using standard thermal cycling conditions with the nucleolin, hnRNP K, VEGF and Actin primers described earlier.

Electrophoretic Mobility Shift Assay (EMSA)

The purification of nucleolin and the electrophoretic mobility shift assay of the recombinant protein and the VG47 oligo was conducted as previously described (12). The plasmid containing the MBP tagged nucleolin was a gift from Dr. Michael B. Kastan (St. Jude Children's Research Hospital, Memphis, TN) (23). To determine the binding of nucleolin to the VEGF G-quadruplex, we used approximately 10 kcpm of the radiolabelled VG47 oligo (Fig.1) and denatured it by heating at 90°C for 5 min, then slow cooled to room temperature with 100 mM KCl to allow the formation of G-quadruplex structures. The folded DNA oligomer was then incubated with increasing amounts of recombinant nucleolin-MBP on ice for 15 minutes to form a protein-DNA complex. The protein-DNA complex was then subjected to a native polyacrylamide gel electrophoresis (PAGE) to separate nucleolin-G-quadruplex complex from unbound DNA by the difference in the electrophoretic mobility. The dissociation constant (Kd) was obtained by quantitating the intensity of the bands by densitometry.

Formation of hnRNPK/DNA Complex and Electrophoretic Mobility Shift Assay and Bromine Footprint

Approximately 50,000 cpm of the purified and labeled VC24 oligo was mixed with 140mM KCl, 50mM NaCl, and 10mM Tris-HCl Buffer at pH 6.5 with or without 250ng of hnRNP K protein for 15 minutes on ice. This mixture was then subject to bromine treatment with 1mM or 2mM Br solution (40μM $KHSO_5$ and 2mM KBr) for 30 minutes at room temperature. The bromine reaction was stopped with 1.5 volume of non-denaturing dye (50% glycerol, 1mg/mL xylene cyanol bromophenol blue) and immediately run in a 12% non-denaturing polyacrylamide gel. The protein-DNA complexed and free-standing DNA bands from the EMSA were then cut from the gel and extracted with 0.4M NH_4OAc, 0.2% SDS, 1mM EDTA, and 1mM $MgCl_2$ and incubated overnight at 37°C. The supernatant was removed and subject to ethanol precipitation/purification and the rest of the experiment was performed according to the non-protein bromine footprint protocol. The recombinant hnRNP K protein was obtained from Amprox (Carlsbad, CA).

RESULTS

C-rich sequence of VEGF promoter forms an i-motif that is pH dependent

Our previous work using CD and bromine footprinting has demonstrated that i-motif structures, with 2:3:2 and 2:3:3 loop configurations, could form within the C-rich strand of the VEGF promoter region under acidic conditions (3). In this study, the stability of these i-

motif structures at physiological pH was further investigated using bromine footprinting at various pH values and bromine concentrations. As previously described (3), the formation of the i-motif structures within the pPu/pPy tract of the VEGF promoter was confirmed in our bromine footprinting experiment using a radiolabelled 24bp oligo containing the VEGF C-rich region (VC24) at both pH 4.3 and 5.3 (Figure 2A). As shown in figure 2A, all four cytosine runs (C3–C6, C9–C11, C15–C17 and C20–C22) were protected from bromination at pH 4.3 and 5.3. Moreover, we found evidence that the VC24 oligomer could form partially unfolded i-motif structures even at a basic pH of 8 (Figure 2A), despite the general view that i-motif structures are not stable at physiological pH. For example, as the pH gradient became more alkaline the 5′ end cytosine runs (C3–C6 and C8–C12) were brominated at a higher rate, however, C9 was completely protected whereas C5 and C4 were partially protected from bromination throughout the pH gradient. Furthermore, the 3′ end cytosine runs (C15–C17 and C20–C22) conserve their bromine protection pattern throughout the pH gradient, with the exception of C19, which was consistently brominated. Three cytosines, highlighted by black solid arrows in figure 2A and 2B, have shown to be conservatively brominated throughout the pH gradient and have been previously noted as loop regions of the VEGF i-motif by their signature sites of high bromination (3). Figure 2B shows schematic representations of the cytosines within the VC24 oligo that are brominated (shown as black circles) or protected from bromination (shown as white circles) according to the footprint shown in figure 2A. The footprint that was produced using the highest bromine concentration within its set of bromine concentration gradient buffers schematically represents each line of black and white circles at each pH level in figure 2B. Furthermore, the models depict an equilibrium of two i-motifs which have 2:3:2 and a 2:3:3 loop configurations that identify C4, C5, C9, C15–C17 and C20–C22 as sites that are protected from bromination throughout the pH gradient highlighted by dotted arrows (Figure 2C). The shift in C-C+ base-pairing between runs C3–C6 to C15–C17 illustrate the increase in bromination of C6 and C3 while C5 and C4 are less susceptible to bromination even at pH 8 (Figure 2C).

hnRNP K and nucleolin bind to the VEGF promoter *in vivo*

Since the identification of Sp1 as a major transcription factor regulating VEGF activity (7, 8) no further efforts have been made to characterize any additional transcription factors interacting within the pPu/pPy tract of the VEGF promoter and that regulate its transcription. This pPu/pPy tract of the VEGF promoter (−85 to −50bp relative to the starting site) has been shown to be a major contributor to transcriptional activity (7, 8). Therefore, we investigated whether hnRNP K and nucleolin could bind to the multi-faceted DNA structures within this tract *in vitro* as well as *in vivo* thus supporting our recent evidence of these two transcription factors binding to the C- and G-rich strands, respectively, of the pPu/pPy tract in the VEGF promoter (12). We also investigated the interaction of CNBP with the pPu/pPy tract of the VEGF promoter since it was known to bind to single-stranded G-rich sequences and act as a transcription factor for the *c-myc* promoter (25) and has been recently reported as a G-quadruplex binding protein (26). Current literature describes Sp1 as a major transcription factor for the VEGF promoter, therefore we used Sp1 as a positive control in our experiments.

We first conducted chromatin immunoprecipitation (ChIP) analysis to determine if hnRNP K and nucleolin, as well as another known G-rich sequence interacting transcription factor (CNBP), could bind directly to the pPu/pPy tract *in vivo*. A498 renal carcinoma cells were used in these experiments with the knowledge that they overexpress VEGF in normoxic conditions (27). After fixing the cells with formaldehyde the DNA-protein complexes were immunoprecipitated using antibodies against hnRNP K, CNBP, nucleolin, Sp1, RNA Pol II, and IgG. We used primers designed to amplify the −242 to +4bp region, relative to the

starting site, which includes the pPu/pPy tract of the VEGF proximal promoter as well as an upstream region of the promoter that contains the hypoxia response element (HRE) to show binding specificity of these transcription factors to the pPu/pPy tract (28). A 290bp band resulted in the case of a successful pull-down of a transcription factor that is complexed with the pPu/pPy tract. As shown in Figure 3A, the samples corresponding to Sp1, hnRNP K and nucleolin pull-down resulted in a significant amplification of the 290bp sequence corresponding to the VEGF proximal promoter region but not for the HRE region. However, CNBP showed the lowest and non-significant amplification of the pPu/pPy region when compared to the band intensity associated with the IgG negative control. As expected, the Sp1 protein showed a strong and specific amplification band corresponding to the pPu/pPy tract. Additionally, these experiments confirmed what was previously observed *in vitro*, in a paper recently published in our lab (12), that nucleolin specifically binds to the VEGF G-rich region *in vivo*.

Determining the effect of hnRNP K and nucleolin expression on VEGF transcription

We investigated whether hnRNP K and nucleolin could regulate VEGF mRNA levels in A498, U251 and HEK293T cells since the *in vivo* binding of these proteins were confirmed via ChIP assay. Therefore, we transfected the described cell lines with siRNA against Nucleolin and hnRNP K. Total mRNA extraction was completed after 48hrs of transfection and was used for semiquantitative RT-PCR. We confirmed mRNA and protein knockdown of each transcription factor by qRT-PCR and Western Blot analysis (Supplemental Figure 1). As shown in figure 4A, the siRNA treatment was capable of a dramatic knockdown of the Nucleolin and hnRNP K mRNA levels in A498, U251 and HEK293T cell lines. Comparison of relative VEGF mRNA levels, upon individual knockdown of Nucleolin or hnRNP K, showed VEGF mRNA levels decreasing around 15% and almost 35% downregulation when both transcription factors are knocked down in A498 cells (Figure 4A). A similar trend is seen in both U251 and HEK293T cells where VEGF mRNA levels drop by an average of 20% when Nucleolin or hnRNP K are individually targeted by siRNA. However, we see an increase or no change in VEGF mRNA levels in U251 and HEK293T cells, respectively, at the highest concentration (100nM) of the combined siRNA treatment (Figure 4B). This unexpected outcome can be due to the increase in recruitment of Sp1 to the pPu/pPy tract that is now predominantly in a double-stranded state, after the double knockdown of nucleolin and hnRNP K, therefore restoring VEGF transcription to basal mRNA levels. It is believed that both nucleolin and hnRNP K shift the equilibrium between B-DNA and non-B-DNA conformations towards the non-B-DNA state by binding and stabilizing G-quadruplex structures and the non-folded state of C-rich sequences, respectively. The overall trend of these knockdown experiments demonstrate that Nucleolin and hnRNP K transcription factors as positive regulators of VEGF transcription. We were unable to completely knockout Sp1 at the mRNA or protein levels (Supplemental Figure 1A & B) however this modest knock-down had the strongest impact on VEGF mRNA levels thus confirming that VEGF transcription (Supplemental Figure1C) is highly sensitive to Sp1 protein levels. Although Sp1 has been well characterized as an important VEGF transcription factor, these experiments demonstrate that the VEGF promoter is also dependent on the transcriptional activation of hnRNP K and nucleolin which are known to bind to non-BDNA conformations. The effect of VEGF mRNA levels upon CNBP siRNA knockdown may indicate indirect effects of CNBP as a transcription factor on genes upstream of the VEGF gene (Supplemental Figure 1C). The regulation of CNBP knockdown at the protein level was not confirmed by western blot as the antibody was not able to detect CNBP protein or it may indicate that the levels of endogenous CNBP are too low for western blot purposes.

Nucleolin binds to the VEGF G-rich sequence and positively regulates its transcription

Nucleolin has been described as a G-quadruplex binding protein by our lab in a recently published article (12), where its high binding affinity to the VEGF G-quadruplex structure was shown though a filter-binding assay. To further examine the role of nucleolin as a positive regulator, we transiently transfected A498, U251 and HEK293T cells with nucleolin and hnRNP K expression vectors to determine the importance of their overexpression in the transcriptional regulation of VEGF through the pPu/pPy tract in its promoter.

Following transient transfections with nucleolin and hnRNP K expression vectors, VEGF mRNA levels were measured using semiquantitative RT/PCR after 48hrs after transfection. As shown in Figure 5A and 5B, elevated VEGF mRNA levels were observed in cells transfected with 500 ng or 1 μg of nucleolin and 1 or 2 μg of hnRNP K expression vectors when compared to cells transfected with 2 μg of empty vector, pEGFP-C3, in all cell lines. In particular, A498 cells showed the highest VEGF mRNA induction, when transfected with nucleolin or hnRNP K expression vector, reaching almost 3 fold compared to the empty vector sample. Although U251 and HEK293T cells were observed to have statistically significant induction of VEGF following transient transfection of nucleolin and hnRNPK expression vectors, U251 had an average of 2 fold expression while HEK293T only obtained 1.5 fold at its highest induction measurement.

Because we have previously shown that nucleolin can physically bind to the VEGF promoter, via the G-quadruplex structure that forms within its pPu/pPy tract (12), we performed an electrophoretic mobility shift assay (EMSA) to demonstrate its binding capability to the VEGF G-rich strand represented in the VG47 oligo. The intensity of the bands in the gel were quantified using densitometry to calculate the dissociation constant (Kd) of nucleolin to VG47 oligo (Figure 5C). The Kd of nucleolin to VG49 oligomer was estimated to approximately 213 nM using the graph form of Kd=[A][B]/[AB] where [A][B]/[AB] is the half point that VG47 oligo has complexed with nucleolin (Figure 5D).

hnRNP K binds to the single-stranded cytosine-rich sequence within the poly (Pu/Py) tract

Lastly, we determined how the formation of the i-motif structure could effect the interaction of hnRNP K, a known cytosine-rich binding transcription factor (17), with the C-rich strand of the VEGF promoter since we confirmed the presence of a pseudo-i-motif structure within the C-rich strand of the VEGF promoter at physiological pH (Figure 2A). The hnRNP K protein is known to bind to C-rich sequences of which some are known to form an i-motif (16, 29) and some that only consist of 12 nucleotides and are not physically capable of forming C-C+ intercalated base-pairing (30). In addition, there has been no previous report as to whether hnRNP K is able to recognize secondary DNA structures, such as the i-motif, that could evolve from C-rich sites. Therefore, we investigated the molecular interactions of hnRNP K with the C-rich strand by determining which cytosine residues within this strand could potentially interact with hnRNP K using EMSA combined with bromine footprinting. In this experiment, the radiolabelled VC24 oligo was treated with Br_2, in the presence or absence of hnRNP K, and its bound or unbound form was separated using PAGE analysis (Figure 6A). The bands corresponding to the bound or unbound state of the VC24 oligo were isolated from the gel and subjected to piperidine cleavage as described in the materials and methods. The cleaved products were then separated on a sequencing gel to determine cytosine specific cleavage sites along side of the purine and pyrimidine sequencing reactions. The cleavage pattern shown in lane I of Figure 6B represents the free oligo treated with 2mM Br_2 without hnRNP K and corresponds to that of the VEGF i-motif footprint observed at pH 7.1 (Figure 2A). The footprinting pattern observed in lane II of Figure 6B, which is the hnRNP K complexed DNA, was quite different from that of the i-motif pattern in lane I, where three specific cytosines (C6, C10 and C19) were completely unprotected in

the free oligo DNA but were protected in lane II. In addition, all four cytosine runs are protected in the hnRNPK-complexed oligo (see lane II of figure 6B) to varying extents. However, lane III that represents the unbound oligo (B) in the presence of hnRNP K does not show protection of any cytosines, suggesting the single-stranded oligo is in an unfolded conformation that is different from that of the free oligo (seen in lane I of figure 6B). The same pattern seen in lanes II and III that is hnRNP K complexed VC24 oligo and treated with 2mM bromine is seen with the samples treated at 1mM bromine. This evidence leads us to suggest that hnRNP K is binding to the VEGF C-rich single-stranded sequence in a different confirmation than that of the i-motif structure so that only three of the four cytosine runs are protected from bromination.

DISCUSSION

There is a growing amount of evidence suggesting the existence of non-B-DNA structures such as G-quadruplexes and i-motifs and their involvement in transcriptional regulation of many human genes, including VEGF (31). In an article recently published in our lab we characterized the G-quadruplex and i-motif structures that form in the G- and C-rich sequences in the pPu/pPy tract of the VEGF promoter (3). In the current study, we further characterized the formation of i-motif structures within a pH gradient spanning pH 4.5 to pH 8 and bromine footprinting analysis (Fig 2). Interestingly, we observed that the two 3′ end cytosine runs are protected throughout the pH gradient, with the exception of one cytosine (e.g. C19). This suggests that this unique protection pattern might be due to the conservation of the basic i-motif structure even at the more basic pH levels, where the C-C+ base-pairing would be weak but sufficient to maintain partially unfolded i-motif structures presumably through base-pair stacking interactions. This model is further supported by the consistent cleavage of cytosines in the predicted loop region (C8, C12 and C19) throughout the pH gradient and this pattern has been shown to be a signature identifier for the VEGF i-motif structure (3). Moreover, these observations indicate that a partially unfolded i-motif structure is sustained at physiological pH such that the loops are kept in a non-paired state and the 3′ end cytosine runs demonstrate cytosine base-pairing. The instability of this partially unfolded i-motif structure could prove to be of importance in prolonging the single-stranded state of the C-rich sequence in the pPu/pPy tract, avoiding its hybridization to the complementary G-rich sequence. Prolonging the single-stranded state of both these sequences can lead to the recruitment of transcription factor proteins that prefer binding to secondary-DNA structures such as the G-quadruplex and the i-motif.

After characterizing the i-motif forming region of the VEGF promoter, we sought to further characterize transcription factor binding to the single-stranded state as well as the G-quadruplex and i-motif states in the G/C-rich promoter region of the VEGF gene. This was necessary as there have been no reports on proteins that influence VEGF transcription via interaction with non-B-DNA structures. The results of our ChIP assay confirmed that the transcription factors, hnRNP K and nucleolin, bind in a sequence specific manner *in vivo* to the pPu/pPy tract of the VEGF proximal promoter (Figure 3). To understand the effect of nucleolin and hnRNP K binding to the VEGF promoter, we knocked down the expression of these proteins in A498, U251 and HEK293T cells (Figure 4). We compared the cancer cell lines A498 and U251, which abnormally express VEGF, with an immortalized embryonic kidney cell line, HEK293T, which normally expresses VEGF. In all cell types, this led to a marginal but statistically significant downregulation of VEGF mRNA levels. When nucleolin and hnRNP K were overexpressed in the same cell lines, VEGF mRNA levels increased by at least two fold (Figure 5). Together, these transient transfection experiments suggest nucleolin and hnRNP K are acting as positive regulators of VEGF transcription. These results led us to design experiments to understand the mechanism of action of these DNA-protein binding interactions and their effect on VEGF transcription.

In our previous studies we characterized the binding of nucleolin to the VEGF and *c-myc* G-quadruplexes in their respective promoters (12), however the DNA-protein interactions in the C-rich sequence of the VEGF promoter are still uncharacterized. With respect to the pPu/pPy tract in the *c-myc* promoter, it is known that hnRNP K preferentially binds to C-rich sequences which can form stable i-motifs (17, 25, 32). Therefore, we were interested in understanding how hnRNP K could potentially bind to the C-rich sequence in the VEGF promoter in the unfolded or i-motif conformation. In order to understand the nature of hnRNP K binding to the unfolded conformation of the C-rich sequence we conducted an EMSA/footprinting experiment. This experiment allowed us to isolate the bound and free oligo species and compare them on a sequencing gel for cytosine protection patterns (Figure 6). The cytosine protection pattern of an i-motif was observed in the EMSA/Footprint of the free C-rich oligo species (lane I in Fig 6b) at pH 6.5. However, the free oligo that was not bound to hnRNP K (lane III of Fig 6b) did not show the i-motif protection pattern, but rather demonstrated a non-specific bromination pattern. The evidence provided in the bromine footprinting patterns suggest that when hnRNP K releases the oligo in a linear state, bromine reacts with the cytosines resulting in a bulky adduct, which could potentially inhibit hnRNP K from reannealing to the oligo or for the oligo to fold back into an partially unfolded i-motif conformation. Therefore, we believe that hnRNP K binds to the oligo via the free cytosine runs in the partially unfolded i-motif formation and either facilitates the unfolding of it to a non-base-paired conformation or traps out the fully single-stranded form of the C-rich oligo.

Based on our results, we have proposed a hypothetical model of how nucleolin and hnRNP K, together with different DNA structural elements, can regulate VEGF promoter transcription (Figure 8). Normally, DNA in the VEGF proximal promoter region exists in duplex form. Sp1, and other double-stranded binding transcription factors, can bind to the VEGF proximal promoter region and activate transcription by associating with transcription initiation proteins to recruit RNA polymerase II. However, when the transcriptional machinery starts to unwind DNA, to begin the RNA polymerase process, the DNA is coiled through the machinery rather than the machinery coiling around the DNA. This DNA unwinding activity begins to negatively supercoil the DNA upstream of this transcriptional event and positively supercoils the DNA downstream of the event. The torsional stress on the negatively supercoiled double-helix allows for atypical DNA structures to form such as G-quadruplexes and i-motifs. Nucleolin can activate transcription by binding to the G-rich strand, presumably in the G-quadruplex structural conformation, and associate with transcription initiation proteins thus recruiting the RNA polymerase complex. In the case of hnRNP K, this transcription factor can either trap out the linear single-stranded C-rich sequence or bind to the non-paired cytosine runs within the partially unfolded i-motif structure and recruit transcription initiation proteins and the RNA polymerase complex to start VEGF transcription. In the present paper, we demonstrated that when both nucleolin and hnRNP K are knocked out, at 100nM combined siRNA concentrations in U251 and HEK293T cells, an increase in VEGF mRNA was observed (Figure 4). The increase in VEGF message was unexpected. We speculate that, in the absence of nucleolin and hnRNP K the atypical secondary DNA structures become unstable and return to the double-stranded DNA state which allows for SP1 binding to occur, thus increasing the VEGF message (Figure 4A). As part of the model building process, we were interested in understanding another G-rich sequence binding protein, CNBP, which is known to bind to G-rich sequences in the linear (25) as well as the G-quadruplex structural conformation (26). Since the ChIP assay (Figure 3) demonstrated a weak binding of CNBP to the VEGF pPu/pPy tract *in vivo*, we believe that CNBP may not be able to bind to the linear single-stranded state of the G-rich sequence because it is in the G-quadruplex structural conformation and nucleolin would have outcompeted CNBP for its binding site. In contrast, transcription initiation of VEGF is prevented through G-quadruplex-interactive agents, such as TMPyP4 and Se2SAP,

which have been shown to bind to the VEGF G-quadruplex and suppress VEGF transcription (33). We hypothesize that the stabilization of the VEGF G-quadruplex by these small-molecules may change the quality of the interactions between the transcription factors, nucleolin and hnRNP K, and the atypical DNA structures within the pPu/pPy tract. The G-quadruplex interacting compounds may also decrease VEGF transcription by driving the structural equilibrium to a G-quadruplex formation within the pPu/pPy tract. While this is interesting speculation, more work needs to be done to fully understand the physical and biological consequence of these small-molecules.

Our hypothetical model of DNA structural transition and the proteins recognizing the different DNA structures in the VEGF proximal promoter not only demonstrates the elegant regulation of expression of the VEGF gene, but also provides a novel way to modulate the transcriptional regulation of VEGF by targeting these atypical DNA secondary structures. These experiments suggest that atypical secondary DNA structures, such as G-quadruplexes and partially unfolded i-motifs, and the transcription factors that recognize and bind to them could play a key role in the regulation of VEGF transcription. Further research will be needed to understand the role of G-quadruplex and i-motif interacting molecules on the binding affinity of nucleolin and hnRNP K to the G- and C-rich sequences of the VEGF pPu/pPy tract. If these small molecules were to interfere with these transcription factor binding sites in the pPu/pPy they could have marked effects on VEGF transcription and in turn could be used for clinical use as anti-angiogenic drugs.

Supplementary Material

Refer to Web version on PubMed Central for supplementary material.

Acknowledgments

We thank Drs. David Bishop and Allison Hays in their contribution to the preparation and editing of the final draft of the text and the figures that are included in this article.

Abbreviations

HIF1-α	hypoxia inducible factor 1 - alpha
Sp1	specificity protein 1
hnRNP K	heterogeneous nuclear ribonucleoprotein K
VEGF	vascular endothelial growth factor
NF-κB	nuclear factor kappa-light-chain-enhancer of activated B cells
HRE	hypoxia response element
pPu/pPy	polypurine/polypyrimidine
ChIP	chromatin immunoprecipitation
siRNA	small interfering RNA
qRT-PCR	quantitative real-time polymerase chain reaction
TBP	TATA-binding protein

Bibliography

1. Cristini V, Frieboes HB, Gatenby R, Caserta S, Ferrari M, Sinek J. Morphologic instability and cancer invasion. Clin Cancer Res. 2005; 11:6772–6779. [PubMed: 16203763]

2. Ferrara N, Kerbel RS. Angiogenesis as a therapeutic target. Nature. 2005; 438:967–974. [PubMed: 16355214]
3. Guo K, Gokhale V, Hurley LH, Sun D. Intramolecularly folded G-quadruplex and i-motif structures in the proximal promoter of the vascular endothelial growth factor gene. Nucleic Acids Res. 2008; 36:4598–4608. [PubMed: 18614607]
4. Kouzine F, Sanford S, Elisha-Feil Z, Levens D. The functional response of upstream DNA to dynamic supercoiling in vivo. Nat Struct Mol Biol. 2008; 15:146–154. [PubMed: 18193062]
5. Wang Y, Patel DJ. Guanine residues in d(T2AG3) and d(T2G4) form parallel-stranded potassium cation stabilized G-quadruplexes with anti glycosidic torsion angles in solution. Biochemistry. 1992; 31:8112–8119. [PubMed: 1525153]
6. Phan AT, Modi YS, Patel DJ. Propeller-type parallel-stranded G-quadruplexes in the human c-myc promoter. J Am Chem Soc. 2004; 126:8710–8716. [PubMed: 15250723]
7. Shi Q, Le X, Abbruzzese JL, Peng Z, Qian CN, Tang H, Xiong Q, Wang B, Li XC, Xie K. Constitutive Sp1 activity is essential for differential constitutive expression of vascular endothelial growth factor in human pancreatic adenocarcinoma. Cancer Res. 2001; 61:4143–4154. [PubMed: 11358838]
8. Finkenzeller G, Sparacio A, Technau A, Marme D, Siemeister G. Sp1 recognition sites in the proximal promoter of the human vascular endothelial growth factor gene are essential for platelet-derived growth factor-induced gene expression. Oncogene. 1997; 15:669–676. [PubMed: 9264407]
9. Abdelrahim M, Smith R 3rd, Burghardt R, Safe S. Role of Sp proteins in regulation of vascular endothelial growth factor expression and proliferation of pancreatic cancer cells. Cancer Res. 2004; 64:6740–6749. [PubMed: 15374992]
10. Stoner M, Wormke M, Saville B, Samudio I, Qin C, Abdelrahim M, Safe S. Estrogen regulation of vascular endothelial growth factor gene expression in ZR-75 breast cancer cells through interaction of estrogen receptor alpha and SP proteins. Oncogene. 2004; 23:1052–1063. [PubMed: 14647449]
11. Abdelrahim M, Safe S. Cyclooxygenase-2 inhibitors decrease vascular endothelial growth factor expression in colon cancer cells by enhanced degradation of Sp1 and Sp4 proteins. Mol Pharmacol. 2005; 68:317–329. [PubMed: 15883203]
12. Gonzalez V, Guo K, Hurley L, Sun D. Identification and characterization of nucleolin as a c-myc G-quadruplex-binding protein. J Biol Chem. 2009; 284:23622–23635. [PubMed: 19581307]
13. Gehring K, Leroy JL, Gueron M. A tetrameric DNA structure with protonated cytosine, cytosine base pairs. Nature. 1993; 363:561–565. [PubMed: 8389423]
14. Kaushik M, Suehl N, Marky LA. Calorimetric unfolding of the bimolecular and i-motif complexes of the human telomere complementary strand, d(C(3)TA(2))(4). Biophys Chem. 2007; 126:154–164. [PubMed: 16822606]
15. Bomsztyk K, Denisenko O, Ostrowski J. hnRNP K: one protein multiple processes. Bioessays. 2004; 26:629–638. [PubMed: 15170860]
16. Lacroix L, Lienard H, Labourier E, Djavaheri-Mergny M, Lacoste J, Leffers H, Tazi J, Helene C, Mergny JL. Identification of two human nuclear proteins that recognise the cytosine-rich strand of human telomeres in vitro. Nucleic Acids Res. 2000; 28:1564–1575. [PubMed: 10710423]
17. Michelotti EF, Michelotti GA, Aronsohn AI, Levens D. Heterogeneous nuclear ribonucleoprotein K is a transcription factor. Mol Cell Biol. 1996; 16:2350–2360. [PubMed: 8628302]
18. Tomonaga T, Levens D. Activating transcription from single stranded DNA. Proc Natl Acad Sci U S A. 1996; 93:5830–5835. [PubMed: 8650178]
19. Brooks TA, Hurley LH. The role of supercoiling in transcriptional control of MYC and its importance in molecular therapeutics. Nat Rev Cancer. 2009; 9:849–861. [PubMed: 19907434]
20. Tataurov AV, You Y, Owczarzy R. Predicting ultraviolet spectrum of single stranded and double stranded deoxyribonucleic acids. Biophys Chem. 2008; 133:66–70. [PubMed: 18201813]
21. Ross SA, Burrows CJ. Cytosine-specific chemical probing of DNA using bromide and monoperoxysulfate. Nucleic Acids Res. 1996; 24:5062–5063. [PubMed: 9016685]
22. Toth J, Biggin MD. The specificity of protein-DNA crosslinking by formaldehyde: in vitro and in drosophila embryos. Nucleic Acids Res. 2000; 28:e4. [PubMed: 10606672]

23. Takagi M, Absalon MJ, McLure KG, Kastan MB. Regulation of p53 translation and induction after DNA damage by ribosomal protein L26 and nucleolin. Cell. 2005; 123:49–63. [PubMed: 16213212]
24. Shanmugam N, Reddy MA, Natarajan R. Distinct roles of heterogeneous nuclear ribonuclear protein K and microRNA-16 in cyclooxygenase-2 RNA stability induced by S100b, a ligand of the receptor for advanced glycation end products. J Biol Chem. 2008; 283:36221–36233. [PubMed: 18854308]
25. Michelotti EF, Tomonaga T, Krutzsch H, Levens D. Cellular nucleic acid binding protein regulates the CT element of the human c-myc protooncogene. J Biol Chem. 1995; 270:9494–9499. [PubMed: 7721877]
26. Borgognone M, Armas P, Calcaterra NB. Cellular nucleic-acid-binding protein, a transcriptional enhancer of c-Myc, promotes the formation of parallel G-quadruplexes. Biochem J. 428:491–498. [PubMed: 20394585]
27. Iwai A, Fujii Y, Kawakami S, Takazawa R, Kageyama Y, Yoshida MA, Kihara K. Down-regulation of vascular endothelial growth factor in renal cell carcinoma cells by glucocorticoids. Mol Cell Endocrinol. 2004; 226:11–17. [PubMed: 15489000]
28. Forsythe JA, Jiang BH, Iyer NV, Agani F, Leung SW, Koos RD, Semenza GL. Activation of vascular endothelial growth factor gene transcription by hypoxia-inducible factor 1. Mol Cell Biol. 1996; 16:4604–4613. [PubMed: 8756616]
29. Fenn S, Du Z, Lee JK, Tjhen R, Stroud RM, James TL. Crystal structure of the third KH domain of human poly(C)-binding protein-2 in complex with a C-rich strand of human telomeric DNA at 1.6 A resolution. Nucleic Acids Res. 2007; 35:2651–2660. [PubMed: 17426136]
30. Valverde R, Edwards L, Regan L. Structure and function of KH domains. FEBS J. 2008; 275:2712–2726. [PubMed: 18422648]
31. Lipps HJ, Rhodes D. G-quadruplex structures: in vivo evidence and function. Trends Cell Biol. 2009; 19:414–422. [PubMed: 19589679]
32. Takimoto M, Tomonaga T, Matunis M, Avigan M, Krutzsch H, Dreyfuss G, Levens D. Specific binding of heterogeneous ribonucleoprotein particle protein K to the human c-myc promoter, in vitro. J Biol Chem. 1993; 268:18249–18258. [PubMed: 8349701]
33. Sun D, Liu WJ, Guo K, Rusche JJ, Ebbinghaus S, Gokhale V, Hurley LH. The proximal promoter region of the human vascular endothelial growth factor gene has a G-quadruplex structure that can be targeted by G-quadruplex-interactive agents. Mol Cancer Ther. 2008; 7:880–889. [PubMed: 18413801]

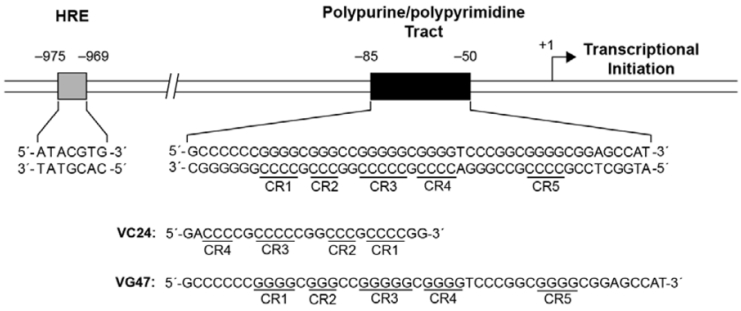

Figure 1. Poly-(Purine/Pyrimidine) tract of the VEGF promoter

A schematic representation of the VEGF proximal promoter demonstrating the position and nucleotide base composition of the hypoxia response element (HRE) and poly-(purine/pyrimidine) tract relative to the transcriptional start site. The six cytosine runs (CR1-5) are underlined in the base composition of the pPu/pPy tract as well as in the sequences of oligonucleotides for orientation. VC24 oligo contains cytosine runs CR4-1 that have been previously characterized to form the i-motif structure. The VG47 is the complimentary strand to VC24, only that it contains the fifth run (CR5) of cytosines on the 5′ end, and was used in EMSA experiments.

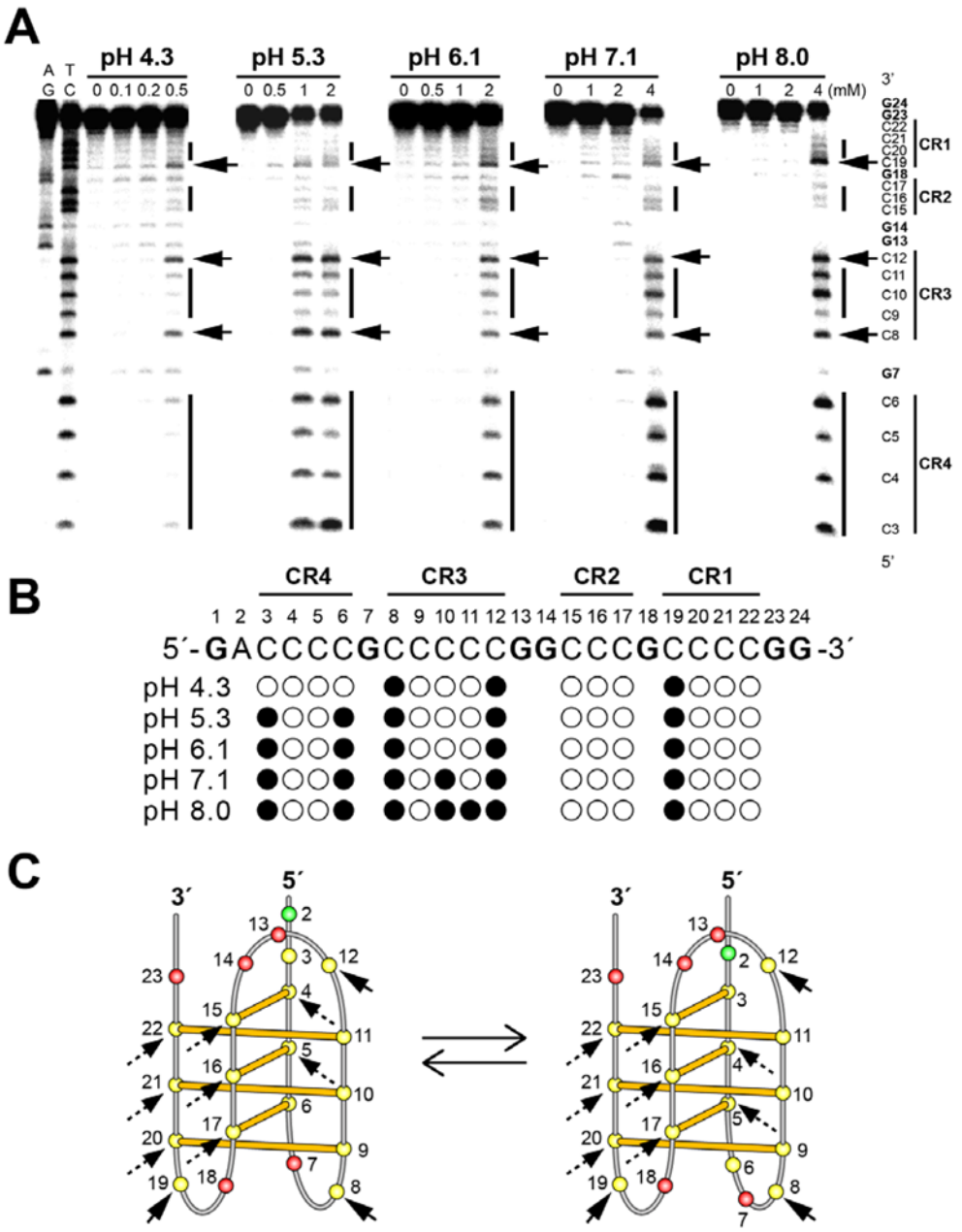

Figure 2. Bromine footprint of oligo VC24 at varying pH

A. Bromine footprinting of VC24 in a gradient of pH buffers each set having three increasing bromine concentrations. The conserved cleavage sites are highlighted with arrows in the sequencing gel and depicted with shaded circles in the schematic representation of VC24 below. B. A schematic representation of the VC24 sequence that represents the four cytosine-rich runs that form the most stable VEGF i-motif. Hyper bromination sites are depicted by black circles at each pH to show the transition of the oligo from the most stable i-motif structure to a less structured form. A schematic diagram of our model for the VEGF i-motif is derived from these experiments.

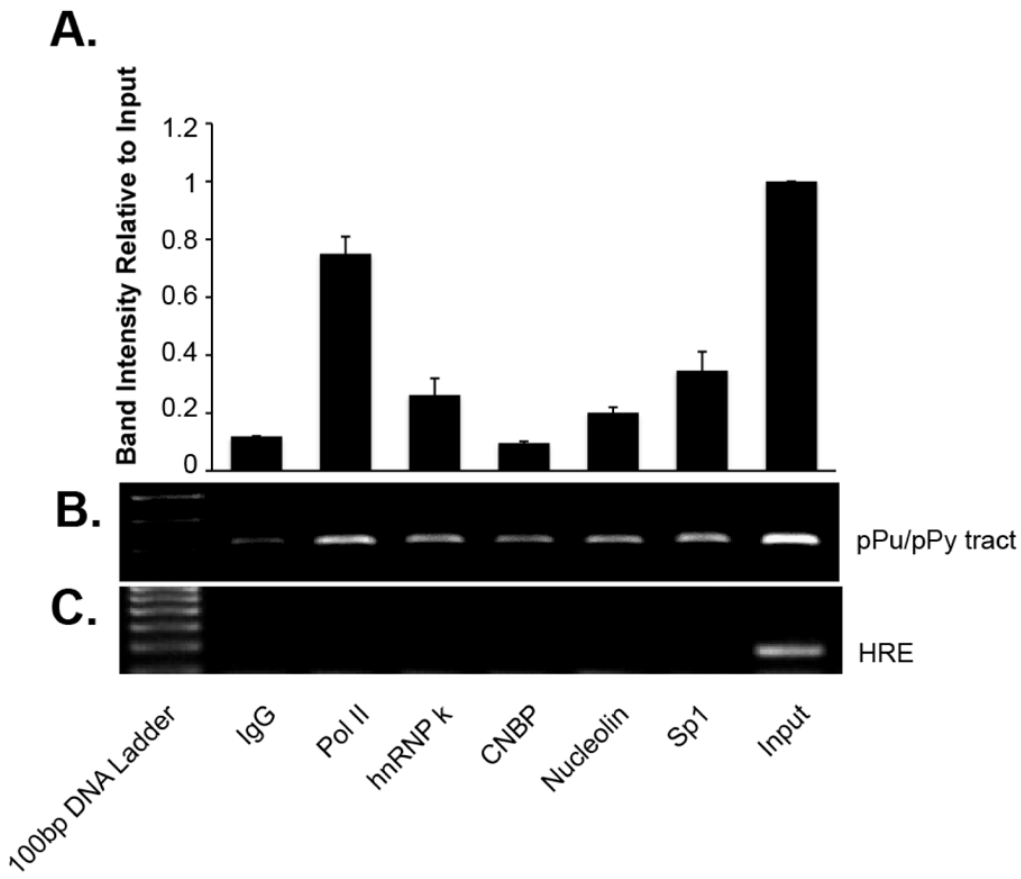

Figure 3. Sp1, nucleolin and hnRNP K bind to the VEGF poly(Purine/Pyrimidine) tract

A. Comparison of band intensity of the results. The bands in three agarose gel analysis corresponding to the poly(Purine/Pyrimidine) tract were scanned in a densitometer and the band intensities were graphed relative to the Input signal. B. & C. An agarose gel analysis of PCR products. Exponentially proliferating A498 cells were harvested for ChIP assay. Protein-DNA cross-linked samples were immunoprecipitated with the indicated antibodies or control IgG, processed, and used as templates for PCR reactions to measure relative amounts of the (B) poly(Purine/Pyrimidine) tract or the (C) HRE region of the genomic VEGF promoter DNA that had been immunoprecipitated. The gel images presented are representative of three independent experiments.

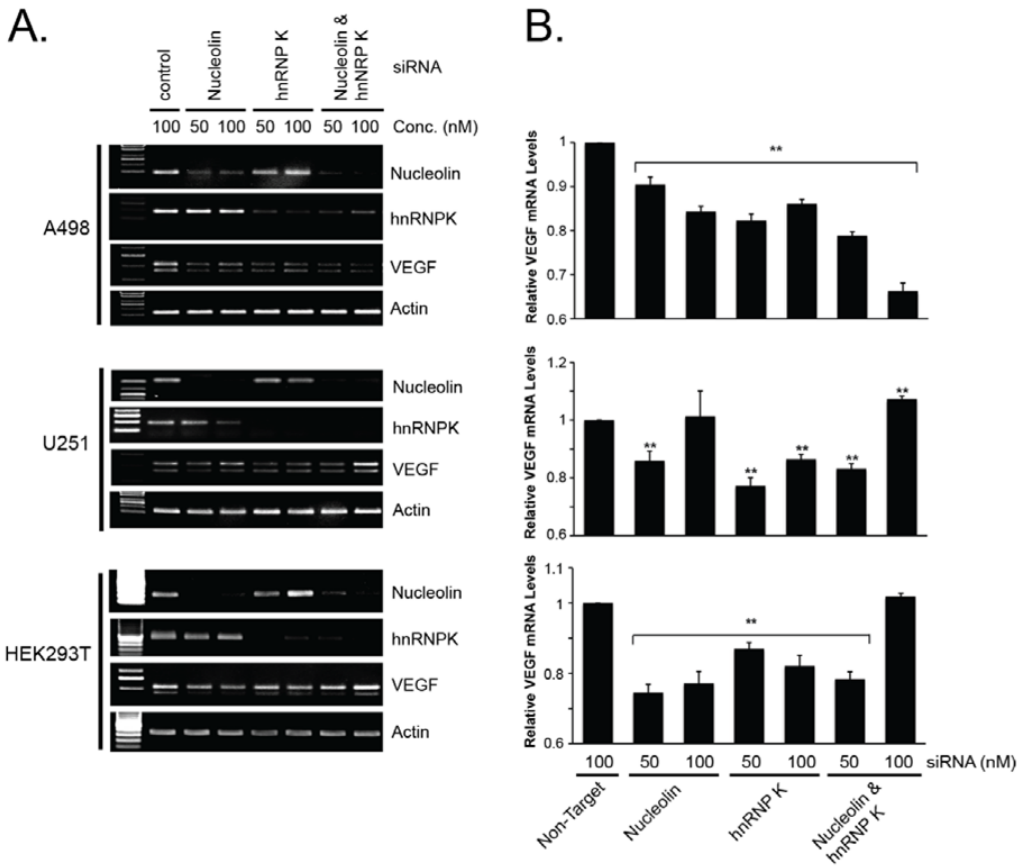

Figure 4. siRNA KO of nucleolin and hnRNP K decreases VEGF mRNA levels

A. Agarose gel analysis of siRNA treated samples. Subconfluent proliferating A498, U251 and HEK293T cells were transiently transfected with non-targeting siRNA (100nM) or nucleolin and hnRNP K targeting siRNA at 50 or 100nM concentrations. 48hrs after transfection total RNA was extracted and was used for semiquantitative RT-PCR. The gel images presented are representative of three independent experiments. B. Quantitative analysis of agarose gel densitometry data. Each PCR band on photographs of the three agarose gels was quantitated using densitometry and are presented as bar graphs relative to control (non-targeting siRNA) means ± S.E. of these values were calculated. Nucleolin and hnRNP K mRNA silencing significantly decreased VEGF mRNA levels ($p < 0.005$ for comparisons of cells transfected with non-targeting siRNA or nucleolin or hnRNP K targeting siRNA). β-Actin was used as the loading control for semiquantitative RT-PCR results.

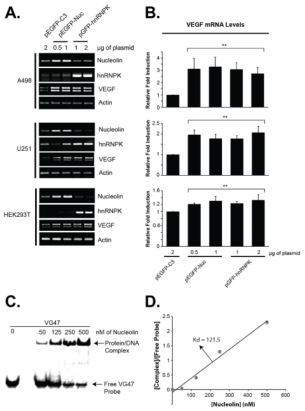

Figure 5. Nucleolin binds to the VEGF G-rich sequence and induces its transcription

A. Agarose gel analysis of cells transiently transfected with nucleolin and hnRNP K expression vectors. Subconfluent proliferating A498, U251 and HEK293T cells were transiently transfected with empty vector (pEGFP-C3) or nucleolin and hnRNP K expression vectors. 48hrs after transfection total RNA was extracted and was used for semiquantitative RT-PCR. The gel images presented are representative of three independent experiments. B. Quantitative analysis of agarose gel densitometry data. Each PCR band on photographs of the three agarose gels was quantitated using densitometry and are presented as bar graphs relative to control (pEGFP-C3) means ± S.E. of these values were calculated. Nucleolin and hnRNP K overexpression significantly enhanced VEGF mRNA expression ($p < 0.005$ for comparisons of cells transfected with or without nucleolin/hnRNP K expression vectors). β-Actin was used as the loading control for semiquantitative RT-PCR results. C. Electrophoresis separation of radiolabelled VG47 complexed with increasing amounts of nucleolin and free oligo. EMSA performed with VG47 probe incubated with increasing amounts of recombinant nucleolin. Protein/DNA complex and free probes are highlighted by arrows at the left of the figure. D. Apparent Kd calculation plot, linear regression of nucleolin concentration versus the concentration of [complex]/[free probe] ratio plot for the EMSA.

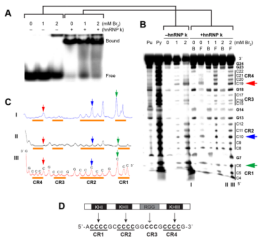

Figure 6. hnRNP K binds to the VEGF pPu/pPy tract sequence and produces a distinct footprint compared to that of the i-motif

A. Electromobility Shift Assay showing radiolabelled VC24 probe subject to 1 or 2mM Bromine reaction with or without 250ng of hnRNP K. Bands at the bottom of the gel are labeled Free (F) for free probe and bands at the top corresponding to hnRNPK-VC24 complex are labeled as Bound (B). B. Bands F and B extracted from the EMSA gel were run in a 20% denaturing acrylamide sequencing gel were it showed a typical i-motif footprint at pH 6.5 in lane 1. Lanes II & III correspond to VC24 probe treated with 2mM Br_2 bound to hnRNPK (B) and free probe (F) where it shows a footprint distinct from that of an i-motif (lane I). C. A histogram showing pixel intensity of bands in lanes I, II and III (C6,10, and 19 respectively) highlighted with orange bars corresponding to the four cytosine runs (CR1 - CR4) starting from 3′ to 5′ Three peaks with three arrows red, blue and green indicating where the i-motif unprotected cytosines in lane I are shown to be protected with the hnRNPK-VC24 complex in lane II. The free standing oligo is shown in lane III where the i-motif signature peaks are diminished compared to that of the nucleotides in the loop region but still present the partially unfolded i-motif structure. D. A schematic view of hnRNP K and its domains and their corresponding binding sites to the VG24 oligo.

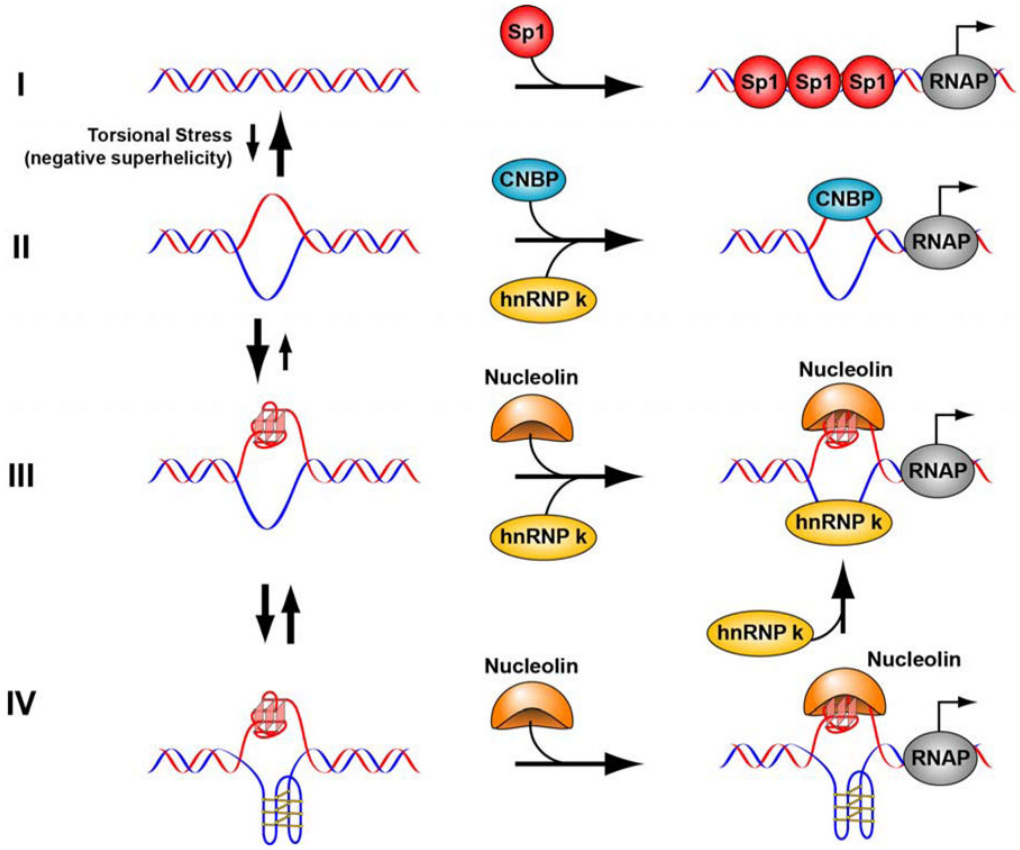

Figure 7. A model showing the structural diversity of the VEGF pPu/pPy tract and its role in transcriptional regulation

I. VEGF transcription can be induced by the conventional transcriptional machinery that is recruited by SP1, a double-stranded (ds) binding transcription factor. II. The transcriptional machinery can also locally unwind a section of the proximal promoter, via superhelicity, that can serve to recruit single-strand (ss) binding transcription factors, CNBP and hnRNP K, consequently turning on transcription. III. The underwound section can induce the formation of a G-quadruplex structure, to relieve torsional stress, thus recruiting nucleolin to recognize and bind to the G-quadruplex structure and hnRNP K to bind to the single-stranded C-rich sequence and recruit RNA Pol II for transcriptional induction. IV. The C-rich strand could also induce the formation of the i-motif along with the G-quadruplex on the opposite G-rich strand. Nucleolin would bind to the G-quadruplex and hnRNP K would either bind to the non-paired cytosine runs in the partially unfolded i-motif where it can further destabilize its structure to a more linear conformation or trap out the linear conformation of the C-rich sequence to further induce transcription.